Next-to-Leading Order Results for $t\bar{t}h$ Production at the Tevatron

L. Reina[1] and S. Dawson[2]

[1]*Physics Department, Florida State University, Tallahassee, Florida 32306*
[2]*Department of Physics, Brookhaven National Laboratory, Upton, New York 11973-5000*

(Received 10 July 2001; published 29 October 2001)

We compute the $\mathcal{O}(\alpha_s^3)$ inclusive total cross section for the process $p\bar{p} \to t\bar{t}h$ in the standard model, at $\sqrt{s_H} = 2$ TeV. The next-to-leading order corrections drastically reduce the renormalization and factorization scale dependence of the Born cross section and slightly decrease the total cross section for renormalization and factorization scales between m_t and $2m_t$.

DOI: 10.1103/PhysRevLett.87.201804 PACS numbers: 14.80.Bn, 12.15.–y, 12.38.Bx, 13.85.–t

Among the most important goals of present and future colliders is the study of the electroweak symmetry breaking mechanism and the origin of fermion masses. If the introduction of one or more Higgs fields is responsible for the breaking of the electroweak symmetry, then at least one Higgs boson should be relatively light, and certainly in the range of energies of present (Fermilab Tevatron) or future [CERN Large Hadron Collider (LHC)] hadron colliders. The present lower bounds on the Higgs mass have been set by CERN Large Electron-Position Collider (LEP) to be $M_h > 114.1$ GeV [1] for the standard model (SM) Higgs boson (h), and $M_{h^0,A^0} > 91$–91.9 GeV [2] for the light scalar (h^0) and pseudoscalar (A^0) Higgs bosons of the minimal supersymmetric standard model (MSSM). At the same time, precision fits to SM results indirectly point to the existence of a light Higgs boson, $M_h <$ 212–236 GeV [3], while the MSSM requires the existence of a scalar Higgs boson lighter than about 130 GeV [4]. Therefore, the possibility of a Higgs boson discovery in the mass range at about 115–130 GeV seems increasingly likely.

In this context, the Tevatron will play a crucial role and will have the opportunity to discover a Higgs boson in the mass range between the experimental lower bound and about 180 GeV [5]. The dominant Higgs production modes at the Tevatron are gluon-gluon fusion, $gg \to h$, and the associated production with a weak boson, $q\bar{q} \to Wh, Zh$. Because of small event rates and large backgrounds, the Higgs search in these channels can be problematic, requiring the highest possible luminosity. It is therefore necessary to investigate all possible production channels, in an effort to fully exploit the range of opportunities offered by the available statistics.

Recently, attention has been drawn to the possibility of detecting a Higgs signal in association with a pair of top-antitop quarks, i.e., in $p\bar{p} \to t\bar{t}h$ [6]. This production mode can play a role over most of the Higgs mass range accessible at the Tevatron. Although it has a small event rate, $\sim$1–5 fb for a SM like Higgs, the signature ($W^+W^- b\bar{b}b\bar{b}$) is quite spectacular. Furthermore, at the Tevatron (unlike at the LHC), the signal and background for this process have quite different shapes. The statistics are too low to allow any direct measurement of the top Yukawa couplings, but recent studies [7] indicate that this channel can reduce the luminosity required for a Higgs discovery at Run II of the Tevatron by as much as 15%–20%.

Up to now the cross section for $p\bar{p} \to t\bar{t}h$ has been known only at tree level. As for any other hadronic process, first-order QCD corrections are expected to be important and are crucial in order to reduce the dependence of the cross section on the renormalization and factorization scales. In this Letter we present the results of our calculation of the next-to-leading-order (NLO) QCD corrections to the total cross section for $p\bar{p} \to t\bar{t}h$ in the standard model, at the Tevatron. A detailed review of the calculation will be presented elsewhere [8]. We find good agreement with the analogous results presented in Ref. [9].

The inclusive total cross section for $p\bar{p} \to t\bar{t}h$ at $\mathcal{O}(\alpha_s^3)$ can be written as

$$\sigma_{\rm NLO}(p\bar{p} \to t\bar{t}h) = \sum_{ij} \int dx_1\, dx_2\, \mathcal{F}_i^p(x_1,\mu)\mathcal{F}_j^{\bar{p}}(x_2,\mu)\hat{\sigma}_{\rm NLO}^{ij}(x_1,x_2,\mu)\,, \tag{1}$$

where $\mathcal{F}_i^{p,\bar{p}}$ are the NLO parton distribution functions for parton i in a proton/antiproton, defined at a generic factorization scale $\mu_f = \mu$, and $\hat{\sigma}_{\rm NLO}^{ij}$ is the $\mathcal{O}(\alpha_s^3)$ parton level total cross section for incoming partons i and j, made of the two channels $q\bar{q}, gg \to t\bar{t}h$, and renormalized at an arbitrary scale μ_r which we also take to be $\mu_r = \mu$. At the Tevatron, for $p\bar{p}$ collisions at hadronic center of mass energy $\sqrt{s_H} = 2$ TeV, more than 95% of the tree level total cross section comes from $q\bar{q} \to t\bar{t}h$, summed over all light quark flavors. Therefore, we compute $\sigma(p\bar{p} \to t\bar{t}h)_{\rm NLO}$ by including in $\hat{\sigma}_{\rm NLO}^{ij}$ only the $\mathcal{O}(\alpha_s)$ corrections to $q\bar{q} \to t\bar{t}h$. The calculation of $gg \to t\bar{t}h$ at $\mathcal{O}(\alpha_s^3)$ is, however, crucial to determine $\sigma_{\rm NLO}(pp \to t\bar{t}h)$ for the LHC, since in pp collisions at $\sqrt{s_H} = 14$ TeV a large fraction of the total cross section comes from the $gg \to t\bar{t}h$ channel. The $\mathcal{O}(\alpha_s^3)$ total cross section for the LHC has been estimated within the effective Higgs approximation in Ref. [10]. Full

results are presented in Ref. [9] and will also appear in Ref. [11].

We write the $\mathcal{O}(\alpha_s^3)$ parton level total cross section as

$$\hat{\sigma}^{ij}_{\rm NLO}(x_1,x_2,\mu) = \alpha_s^2(\mu)\left\{\hat{f}^{ij}_{\rm LO}(x_1,x_2) + \frac{\alpha_s(\mu)}{4\pi}\hat{f}^{ij}_{\rm NLO}(x_1,x_2,\mu)\right\} \equiv \hat{\sigma}^{ij}_{\rm LO}(x_1,x_2,\mu) + \delta\hat{\sigma}^{ij}_{\rm NLO}(x_1,x_2,\mu), \quad (2)$$

where $\alpha_s(\mu)$ is the strong coupling constant renormalized at the arbitrary scale $\mu_r = \mu$, $\hat{\sigma}^{ij}_{\rm LO}(x_1,x_2,\mu)$ is the $\mathcal{O}(\alpha_s^2)$ Born cross section, and $\delta\hat{\sigma}^{ij}_{\rm NLO}(x_1,x_2,\mu)$ consists of the $\mathcal{O}(\alpha_s)$ corrections to the Born cross section. The Born cross section $\hat{\sigma}^{ij}_{\rm LO}(x_1,x_2,\mu)$ has a strong μ dependence, which is canceled at NLO by $\delta\hat{\sigma}^{ij}_{\rm NLO}(x_1,x_2,\mu)$, up to the term of $\mathcal{O}(\alpha_s^4)$. The resulting NLO cross section is therefore much more stable under variations of μ, as will be discussed in the following (see also Fig. 3 below).

$\delta\hat{\sigma}^{ij}_{\rm NLO}(x_1,x_2,\mu)$ contains both $\mathcal{O}(\alpha_s)$ virtual and real corrections to the lowest-order cross section and can be written as the sum of two terms:

$$\delta\hat{\sigma}^{ij}_{\rm NLO}(x_1,x_2,\mu) = \hat{\sigma}^{ij}_{\rm virtual} + \hat{\sigma}^{ij}_{\rm real} = \int d(PS_3)M(ij\to t\bar{t}h) + \int d(PS_4)M(ij\to t\bar{t}h + g), \quad (3)$$

where $M(ij\to t\bar{t}h)$ and $M(ij\to t\bar{t}h + g)$ are, respectively, the matrix elements squared for the $\mathcal{O}(\alpha_s^3)$ $2\to 3$ and $2\to 4$ processes averaged over the initial degrees of freedom and summed over the final ones, while $d(PS_3)$ and $d(PS_4)$ denote the integration over the corresponding three/four particle phase space.

The $\mathcal{O}(\alpha_s)$ virtual corrections to the tree level $q\bar{q}\to t\bar{t}h$ process consist of self-energy, vertex, box, and pentagon diagrams. The calculation of the virtual diagrams was performed by using dimensional regularization in $d = 4 - 2\epsilon$ dimensions. The diagrams have been evaluated by using FORM [12] and MAPLE, and all tensor integrals have been reduced to linear combinations of a fundamental set of scalar integrals. We computed analytically all scalar integrals which give rise to either ultraviolet or infrared singularities, while finite scalar integrals were evaluated using standard packages [13].

Box and pentagon diagrams are ultraviolet finite, but have infrared divergences. The calculation of many scalar box integrals and in particular of the scalar pentagon integrals is extremely laborious, due to the large number of massive particles present in the final state. We evaluated the necessary pentagon scalar integrals by using the method of Ref. [14], and the analytic results are presented in Ref. [8].

Self-energy and vertex diagrams contain both infrared and ultraviolet divergences. The ultraviolet divergences are renormalized by introducing a suitable set of counterterms. Since the cross section is a renormalization group invariant, we need only to renormalize the wave function of the external fields, the top quark mass, and the coupling constants. We use on-shell subtraction for the wave-function renormalization of the external fields. We define the top mass counterterm in such a way that m_t is the pole mass. This counterterm must be used twice: (i) to renormalize the top quark mass, and (ii) to renormalize the top-quark Yukawa coupling. Finally, for $\alpha_s(\mu)$ we use the $\overline{\rm MS}$ scheme, modified to decouple the top quark [15]. The first n_{lf} light fermions are subtracted using the $\overline{\rm MS}$ scheme, while the divergences associated with the heavy quark loop are subtracted at zero momentum.

The $\mathcal{O}(\alpha_s)$ corrections to the Born cross section due to real gluon emission have been computed using a two-cutoff implementation of the phase-space slicing algorithm [16]. The contributions to $q\bar{q}\to t\bar{t}h + g$ are first divided into a soft and a hard contribution,

$$\hat{\sigma}^{q\bar{q}}_{\rm real} = \hat{\sigma}_{\rm soft} + \hat{\sigma}_{\rm hard}, \quad (4)$$

where "soft" and "hard" refer to the energy of the radiated gluon. This division into hard and soft contributions depends on an arbitrary soft cutoff, δ_s, such that the energy E_g of the radiated gluon in the $q\bar{q}$ center-of-mass (c.m.) frame is considered soft if $E_g \le \delta_s\frac{\sqrt{s}}{2}$, where $\sqrt{s}$ is the partonic center of mass energy. The cutoff δ_s must be very small, such that the terms of order δ_s can be neglected. Therefore, to evaluate the soft contribution, the eikonal approximation to the matrix elements can be taken and the integral over the soft degrees of freedom performed analytically.

The hard contribution to $q\bar{q}\to t\bar{t}h + g$ is further divided into a hard/collinear ($\hat{\sigma}_{\rm hard/coll}$) and a hard/noncollinear region ($\hat{\sigma}_{\rm hard/noncoll}$). The hard/collinear region is defined as the region where the energy of the gluon is $E_g > \delta_s\frac{\sqrt{s}}{2}$ and the gluon is radiated from the initial massless quarks at an angle θ_{ig} ($i = q,\bar{q}$), in the $q\bar{q}$ center-of-mass frame, such that $(1 - \cos\theta_{gi}) \le \delta_c$, for an arbitrary small collinear cutoff δ_c. The matrix element squared in the hard/collinear limit is found by using the leading pole approximation, and the integration over the angular degrees of freedom is performed analytically. The hard gluon emission from the final massive quarks never belongs to the hard/collinear region. The contribution from the hard/noncollinear region is finite and is computed numerically, using standard Monte Carlo techniques.

$\hat{\sigma}_{\rm soft}$ and $\hat{\sigma}_{\rm hard/coll}$ contain IR singularities, which are calculated using dimensional regularization, and cancel ex-

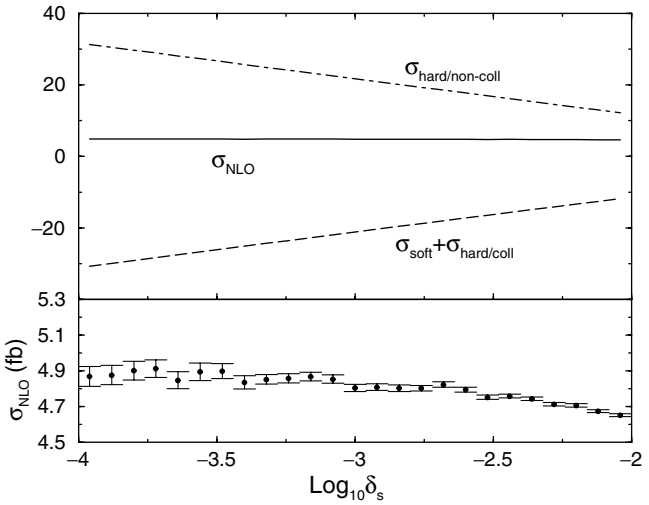

FIG. 1. Dependence of $\sigma_{\rm NLO}(p\bar{p} \to t\bar{t}h)$ on the soft cutoff δ_s, at $\sqrt{s_H} = 2$ TeV, for $M_h = 120$ GeV, $\mu = m_t$, and $\delta_c = 10^{-4}$. The lower scale shows the statistical error on $\sigma_{\rm NLO}$.

actly the analogous singularities from the virtual contributions, after mass singularities have been absorbed in the renormalized parton distribution functions.

Both $\hat{\sigma}_{\rm soft}$ and $\hat{\sigma}_{\rm hard}$ depend on the two arbitrary cutoffs δ_s and δ_c, but the the real hadronic cross section, $\sigma_{\rm real}$, after mass factorization, is cutoff independent. The cutoff independence of the NLO cross section, $\sigma_{\rm NLO}$, is shown explicitly in Figs. 1 and 2. We note that $\sigma_{\rm NLO}$ also includes the contributions from the $\mathcal{O}(\alpha_s)$ virtual corrections and the Born cross section. Since these two terms are cutoff independent, we do not plot them explicitly in the upper part of Figs. 1 and 2. In Fig. 1, we show the dependence of $\sigma_{\rm NLO}$ on the soft cutoff, δ_s, for a fixed value of the collinear cutoff, $\delta_c = 10^{-4}$. In the upper window we illustrate the cancellation of the δ_s dependence between $\sigma_{\rm soft} + \sigma_{\rm hard/coll}$ and $\sigma_{\rm hard/noncoll}$, while in the lower window we show $\sigma_{\rm NLO}$ with the statistical errors

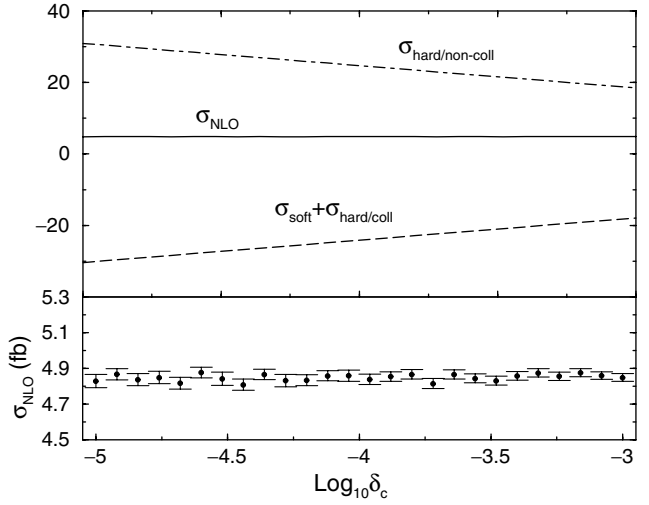

FIG. 2. Dependence of $\sigma_{\rm NLO}(p\bar{p} \to t\bar{t}h)$ on the collinear cutoff δ_c, at $\sqrt{s_H} = 2$ TeV, for $M_h = 120$ GeV, $\mu = m_t$, and $\delta_s = 5 \times 10^{-4}$. The lower scale shows the statistical error on $\sigma_{\rm NLO}$.

from the Monte Carlo integration. For δ_s in the range 10^{-4}–2.5×10^{-2}, a clear plateau is reached and the result is independent of δ_s. Analogously, Fig. 2 shows the independence of $\sigma_{\rm NLO}$ on the collinear cutoff, δ_c, for a fixed value of the soft cutoff, $\delta_s = 5 \times 10^{-4}$: a clear plateau is reached for δ_c in the range 10^{-5}–10^{-3}. All the results presented in the following are obtained using δ_s and δ_c in the range 10^{-4}–10^{-3}.

Our numerical results are found using CTEQ4M parton distribution functions for the calculation of the NLO cross section, and CTEQ4L parton distribution functions for the calculation of the lowest-order cross section [17]. The NLO (LO) cross section is evaluated using the two-(one-)loop evolution of $\alpha_s(\mu)$. The top quark mass is taken to be $m_t = 174$ GeV and $\alpha_s^{\rm NLO}(M_Z) = 0.116$.

In Fig. 3 we show, for $M_h = 120$ GeV, how at NLO the dependence on the arbitrary renormalization/factorization scale μ is significantly reduced. We notice that only for scales μ of the order of $2m_t + M_h$ or bigger is the NLO result greater than the lowest-order result, at $\sqrt{s_H} = 2$ TeV.

Figure 4 shows both the LO and the NLO total cross section for $p\bar{p} \to t\bar{t}h$ at $\sqrt{s_H} = 2$ TeV, as functions of M_h, for two values of the renormalization scale $\mu = m_t$ and $\mu = 2m_t$. Over the entire range of M_h accessible at the Tevatron, for scales $m_t \le \mu \le 2m_t$, the NLO corrections decrease the rate. For example, for $M_h = 120$ GeV and $\mu = m_t$ the NLO total cross section is reduced to 4.86 ± 0.03 fb from the lowest-order prediction of 6.868 ± 0.002 fb. The reduction is much less dramatic at $\mu = 2m_t$, as can be seen from both Figs. 3 and 4. The error we quote on our values is the statistical error on the numerical integration involved in evaluating the total cross section. We estimate the remaining theoretical error to be about 12%, mainly due to the residual μ dependence, to the parton distribution functions, and to the experimental error on m_t.

The corresponding K factor, $K = \sigma_{\rm NLO}/\sigma_{\rm LO}$, i.e., the ratio of the NLO cross section to the LO cross section,

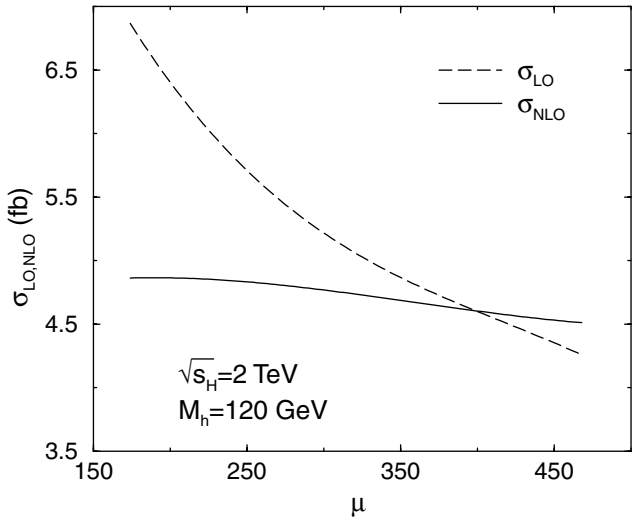

FIG. 3. Dependence of $\sigma_{\rm LO,NLO}(p\bar{p} \to t\bar{t}h)$ on the renormalization scale μ, at $\sqrt{s_H} = 2$ TeV, for $M_h = 120$ GeV.

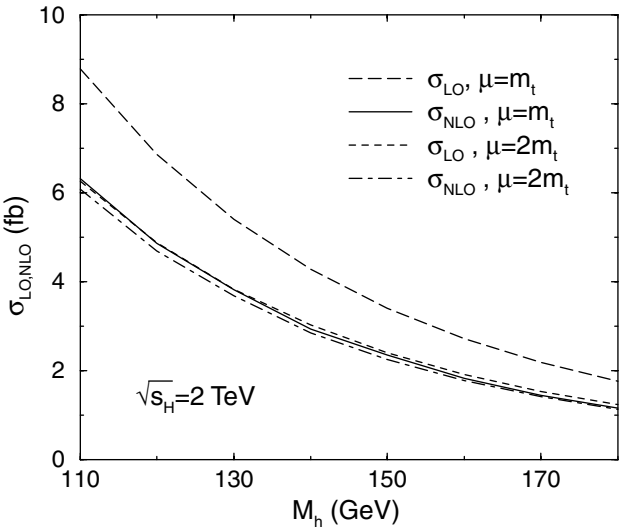

FIG. 4. $\sigma_{\rm NLO}$ and $\sigma_{\rm LO}$ for $p\bar{p} \to t\bar{t}h$ as functions of M_h, at $\sqrt{s_H} = 2$ TeV, for $\mu = m_t$ and $\mu = 2m_t$.

is shown in Fig. 5. Given the strong scale dependence of the LO cross section, the K factor also shows a significant μ dependence, while it is almost constant with M_h. For scales μ between $\mu = m_t$ and $\mu = 2m_t$, the K factor varies roughly between $K = 0.70$ and $K = 0.95$. The reduction of the NLO cross section with respect to the Born cross section is due to the fact that at $\sqrt{s_H} = 2$ TeV the $t\bar{t}h$ final state is produced in the threshold region. In this region the gluon exchange between the final state quarks gives origin to Coulomb singularities that contributes to the cross section with terms of order α_s/β, where β is the velocity of the top-antitop quark in the $t\bar{t}$ c.m. frame. Since the $t\bar{t}h$ final state is in a color-octet configuration, these corrections are negative and therefore contribute to decrease the Born cross section, causing the K factor to

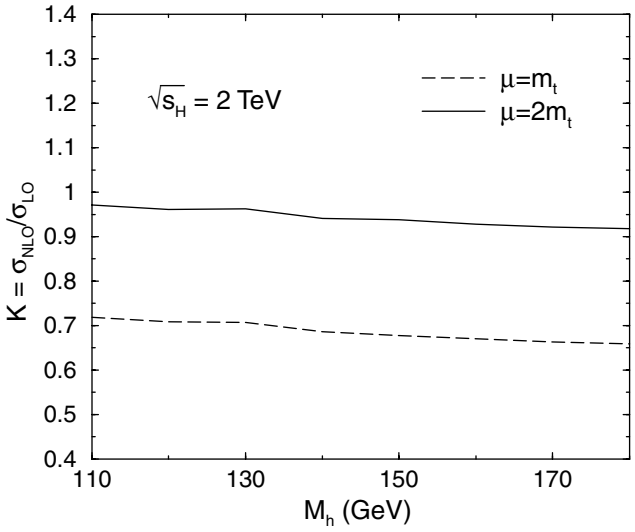

FIG. 5. K factor for $p\bar{p} \to t\bar{t}h$ as a function of M_h, at $\sqrt{s_H} = 2$ TeV, for $\mu = m_t$ and $\mu = 2m_t$.

be smaller than unity. The same effect was observed in the NLO cross section for $e^+e^- \to t\bar{t}h$ [18]. In that case, however, the $t\bar{t}h$ final state is in a color-singlet configuration and the threshold corrections are positive.

The NLO QCD corrections to the standard model process $p\bar{p} \to t\bar{t}h$, at $\sqrt{s_H} = 2$ TeV, reduce the LO cross section by a factor of 0.7–0.95 for renormalization and factorization scales $m_t \le \mu \le 2m_t$, while they slightly increase the LO cross section for scale of the order of $2m_t + M_h$ or larger. The NLO result shows a drastically reduced scale dependence as compared to the Born result and leads to increased confidence in predictions based on these results.

We thank Z. Bern, F. Paige, and D. Wackeroth for valuable discussions and encouragement. We are grateful to the authors of Ref. [9] for detailed comparisons of results prior to publication. The work of L. R. (S. D.) is supported in part by the U.S. Department of Energy under Grant No. DE-FG02-97ER41022 (DE-AC02-76CH00016).

[1] LHWG Note/2001-03, Report No. CERN-EP/2001-055, 2001.
[2] LHWG Note/2001-04, 2001.
[3] LEPEWWG/2001-01, 2001.
[4] S. Heinemeyer, W. Hollik, and G. Weiglein, Eur. Phys. J. C **9**, 343 (1999).
[5] M. Carena *et al.,* hep-ph/0010338.
[6] J. Goldstein, C. S. Hill, J. Incandela, S. Parke, D. Rainwater, and D. Stuart, Phys. Rev. Lett. **86**, 1694 (2001).
[7] J. Incandela, in Proceedings of the Workshop on the Future of Higgs Physics, Fermilab, 2001 (to be published).
[8] L. Reina, S. Dawson, and D. Wackeroth, Reports No. FSU-HEP-2001-0602, No. BNL-HET-01/19, No. UR-1639, hep-ph/0109066.
[9] W. Beenakker, S. Dittmaier, M. Krämer, B. Plümper, M. Spira, and P. Zerwas, following Letter, Phys. Rev. Lett. **87**, 201805 (2001).
[10] S. Dawson and L. Reina, Phys. Rev. D **57**, 5851 (1998).
[11] S. Dawson, L. Orr, L. Reina, and D. Wackeroth (to be published).
[12] J. A. M. Vermaseren, math-ph/0010025.
[13] G. J. van Oldenborgh and J. A. Vermaseren, Z. Phys. C **46**, 425 (1990).
[14] Z. Bern, L. Dixon, and D. A. Kosower, Phys. Lett. B **302**, 299 (1993); Phys. Lett. B **318**, 649E (1993); Nucl. Phys. **B412**, 751 (1994).
[15] J. Collins, F. Wilczek, and A. Zee, Phys. Rev. D **18**, 242 (1978); W. J. Marciano, Phys. Rev. D **29**, 580 (1984); Phys. Rev. D **31**, 213E (1984).
[16] B. W. Harris and J. F. Owens, hep-ph/0102128; U. Baur, S. Keller, and D. Wackeroth, Phys. Rev. D **59**, 013002 (1999).
[17] CTEQ Collaboration, H. L. Lai *et al.,* Phys. Rev. D **55**, 1280 (1997).
[18] S. Dittmaier, M. Kramer, Y. Liao, M. Spira, and P. M. Zerwas, Phys. Lett. B **441**, 383 (1998).